MRS Communications (2018), *8*, 1363–1370
© Materials Research Society, 2018
doi:10.1557/mrc.2018.183

MRS Communications

Research Letter

Modification with ultrasonication for enhanced properties of cobalt-based zeolitic imidazolate framework

Shuyang Sun, Pengcheng Wang, and **Ming Lu,** School of Chemical Engineering, Nanjing University of Science and Technology, Nanjing 210094, Jiangsu Province, People's Republic of China

Address all correspondence to Lu Ming at **luming@njust.edu.cn**

(Received 17 May 2018; accepted 15 August 2018)

Abstract

Effective modification of existing supported catalyst has attracted plenty of interests recently. Herein, we introduced ultrasonication to synthesize the palladium-loaded cobalt-based zeolitic imidazolate framework and compared its properties with those using the conventional method. Remarkably, the ultrasonicated frameworks possess 15.33% higher of Brunauer–Emmett–Teller (BET) surface area and 63.37% higher of *t*-plot external surface area, respectively, which lead up to 23% rise in the degradation of organic pollutants under optimized conditions. Characterizations clearly revealed the causality between ultrasonication, morphology, and catalytic performance compared with their non-ultrasonicated counterparts which further demonstrates a simple but useful method for the modification of supported catalysts.

Introduction

Metal–organic frameworks (MOFs), an advanced type of porous materials with three-dimensional structures, have attracted increased interest.[1] In particular, metal nanoparticles-loaded MOFs (MNPs-MOFs) provide numerous advantages, synergistically combining all the properties of components for multifunctional applications[2,3] and often exhibiting performances superior to those of individual materials and frameworks, meanwhile being promising for controlling or enhancing nanoparticles' (NPs) properties.[4]

As a subfamily of MOFs material, zeolitic imidazolate frameworks (ZIFs) exhibit similar but unique structures where the metal ions (e.g., Zn^{2+} and Co^{2+}) are linked through the nitrogens of the coordinates (usually are deprotonated imidazolate residues) which are easier to synthesize. In general, zeolite frameworks are prepared by solvothermal techniques or adding ultrasonication to the synthesis process, which fasten the nucleation reactions by acoustically generating heat and pressure , has been explored to shorten the synthesis time.[5,6] ZIFs are comprising of channel structure with pores and cages, which define their chemical and physical properties.[7] The structure of common ZIFs mostly influenced by ligands, metal clusters, as well as synthesis conditions in which they created.[8] Compared with most MOFs, ZIFs possess sturdy porosity, excellent thermal and chemical stability, being particularly promising as framework supports for MNP immobilization. However, MNPs tend to aggregate during synthesizing and reaction process due to their high surface energy, resulting in the deactivation of the corresponding catalysts.[9–11] Since the inhibition of MNP agglomeration during catalytic synthesizing and reactions depends on the corresponding fabrication strategy, MNPs loaded onto the surface of ZIFs or inside ZIF pores (MNP-ZIF composites) are considered promising catalysts. The pores in ZIF structure are expected to control MNPs to grow, migrate, and aggregate when loading in confined cavities, which is of great importance for their use as nano-catalyst frameworks.

Catalytic reactions from aromatic nitro-compounds to aromatic amino compounds conform to the growing requirements of green chemistry. Because of the nitro groups are usually inert, the reduction of the nitroaromatic derivatives are difficult to react spontaneously with reductants under room temperature and atmospheric pressure.[12] Ece Tugba Saka[13] researched Co(II) as phthalocyanine complex catalysts used for the degradation of organic (mainly nitro aromatic derivatives) pollutants. Using mesoporous structures as support for MNPs is another approach to the solution.[14,15] However, developing new and efficient structures of the catalyst is of great difficulty. Simple and effective modification methods such as introducing ultrasonication and microwave to the reaction system can make a tremendous change.

Today, ultrasonication is regarded as an effective way in a chemical reaction to accelerate the mass transfer process. With the frequency of 20 kHz–10 MHz,[16] the sonic waves induce the acoustic streaming and create microscopic turbulence throughout the system and induces acoustic cavitation.[17] The micrometrical bubbles in liquids grew and collapsed, which concomitantly enhance chemical activities. There are

https://doi.org/10.1557/mrc.2018.183 Published online by Cambridge University Press

three categories of sonochemical reactions: ultrasonication of liquids (homogeneous), ultrasonication of liquid–liquid or solid–liquid systems (heterogeneous) and direct sonocatalysis. Heterogeneous sonochemistry was widely used to prepare NPs and MOFs such as Ni-BTC (MOF-5),[18] Cu-BTC (HKUST-1),[19] Si-ZIF (zeolite T),[7] and Fe(III)-based MOFs.[20] By breaking intermolecular interactions, ultrasonication was used to speed dissolution, dispersing NPs more evenly in liquids and accelerate the reaction of forming frameworks. Razavi et al. studied the synthesis of TMU-34(-2H) of ultrasonication, which is a functionalized MOF used to detect phenylhydrazine.[21] By changing sonication time, power, and other parameters, the synthesizing process was optimized and the product showed much higher detection limit and shorter response time than the conventional product. Nadar and Rathod introduced ultrasonic treatment to lipase within ZIF-8 and the activity raised to 1.6-folds.[22] By using sonochemical techniques, Abuzalat et al. successfully designed a new way to make the MOF films grow on surfaces of sensors[23] for gas. The modified organic frameworks with ultrasonic irradiation have greater efficiency on the removal and degrading dyes.[24,25] Rakhi[26] compared different ultrasonication methods for intensifying oxalic acid crystallization. Magneto-sonochemical dissociation was another approach to employ ultrasonic with magnetic mechanisms as an efficiency way to improve. Water pollutants, especially chlorinated-organic compounds, can be decomposed directly with ultrasonic irradiation.[27]

In this work, the Co-based ZIF (ZIF-67 derivatives) was synthesized under ultrasonication (ZIF-67-US) followed by loading Pd NPs which was also to use ultrasonic irradiation to obtain Pd-ZIF-67-US products. The synthesized products were further tested as a catalyst in the degradation of nitro aromatic pollutants. Ultrasonication was used to speed up the formation and modify the surface of ZIF-67 frameworks, and break up aggregates of Pd NPs to obtain a better Pd loading on the surface of the modified framework. Since most investigations of ultrasonication-modified process mainly focus on the yields of catalytic reactions[28,29] and general performances of synthesized catalysts,[30,31] we herein took a step forward to compare the ultrasonicated products with the conventional ones from the frameworks to the final modified catalysts, and determine the effects of ultrasonication on surface morphology by performing x-ray diffraction (XRD), scanning electron microscopy (SEM), transmission electron microscopy (TEM), and N_2 sorption using Brunauer–Emmett–Teller (BET) method. Moreover, the catalytic performance was evaluated in the reduction of organic pollutants (nitrobenzene derivatives) with formic acid, used as a hydrogen source, under atmospheric pressure and mild conditions to reveal the causality between ultrasonication and catalytic activity. Despite the main issue of ZIFs that the adsorption of water along with CO_2, we optimized the synthesis and reaction conditions to avoid the interaction with water. The simple approach endows the ultrasonication-modified catalysts with better catalytic activity in the reduction reaction of nitrobenzenes pollutants.

Chemicals and experimental

Chemicals

All chemical materials used in the research were as received without further purification. 2-Methylimidazole (2-MeIm; 99%), $Co(NO_3)_2{\cdot}6H_2O$, and $Pd(CH_3COO)_2$ (Pd > 47%), 4-nitroaniline, 4-nitrophenol, 4-nitroanisole, were supplied by Adamas Reagent Co., Ltd. Nitrobenzene and 2,4-dinitrochlorobenzene, 4-nitrobenzaldehyde, o/m-chloronitrobenzene were supplied by Xiya Reagent Co., Ltd. p-Chloronitrobenzene was supplied by Aladin Industrial Corporation. Polyvinylpyrrolidone, m/p-nitrotoluene were supplied by Sinopharm Chemical Reagent Co., Ltd. 2,4- and 2,6-Dinitrotoluenes were supplied by Shanghai Darui Finechemical Co., Ltd.

All solvents (methanol, ethanol, DMF, acetonitrile, petroleum ether, ethyl acetate, etc.) were supplied by Shanghai Titan Scientific Co., Ltd.

Synthesis of ZIF-67-US and Pd-ZIF-67-US

In this synthesis procedure,[32] 4 mmol $Co(NO_3)_2{\cdot}6H_2O$ (1.164 g) was dissolved in methanol (20 mL) and 16 mmol 2-MeIm (1.312 g) was dissolved in methanol (40 mL) at ambient temperature. Subsequently, the 2-MeIm solution was mixed with the Co(II) solution dropwise under ultrasonic bath to obtain a purple homogeneous solution that was left to react for a certain period (10 min to 6 h). The dark purple solid product was then collected by centrifugation, washed with methanol and ethanol several times, and finally dried at 70°C overnight to obtain crystals of synthesized ZIF-67-US.

To prepare Pd-ZIF-67-US, $Pd(CH_3COO)_2$ (20 mg) was dissolved in acetone (10 mL) to obtain an orange solution, which was treated with as-synthesized ZIF-67 (50 mg) under ultrasonic bath at 56°C for an hour to form a homogeneous solution. Subsequently, formic acid (500 µL) was slowly injected into the mixture, and the obtained dark solids were collected by centrifugation, washed the products with acetone for several times, and dried overnight at 70°C to obtain the synthesized Pd-ZIF-67-US.

Synthesis of conventional ZIF-67 and Pd-ZIF-67

To prepare the conventional ZIF-67 and Pd-loaded ZIF-67, all raw materials and synthesizing processes were set to the same as in synthesizing the ultrasonication-supported ZIF-67-US and Pd-loaded ZIF-67-US. Instead of an ultrasonic bath during the whole process, magnetic stirring and water bath with the corresponding temperature were used.

Hydrogenation of nitro-aromatic derivatives

Liquid-phase hydrogenation of nitrobenzene derivatives with formic acid (HCOOH) as a hydrogen source is widely used as a template reaction to estimate the performances of the target catalysts. Herein, the reduction reaction was carried out using DMF as solvent at 60°C (in a water bath) in a three-necked flask with magnetic stirring.

https://doi.org/10.1557/mrc.2018.183 Published online by Cambridge University Press

Typically, 2 mmol selected nitrobenzene derivative was dissolved in 20 mL of DMF and transferred into the three-necked flask, followed by adding 20 mg of the as-synthesized catalyst under magnetic stirring. The reaction system was heated up to 60°C, and HCOOH (500 μL) was injected into the reaction mixture. The system was kept at 60°C for a certain period and monitored by thin layer chromatography, using ethyl acetate and petroleum ether (1 : 5, volume ratio) as developing solvent. Samples with different reaction time were reserved and their conversion and selectivity were finally monitored by high-performance liquid chromatography (HPLC) using acetonitrile as the mobile phase.

In the stability tests, modified catalysts were recovered after each run by centrifugation, sequentially washed with methanol and acetone several times, and used in the next run with exactly the same conditions.

Optimization

To optimize the parameters in the degradation reactions, the reduction of nitrobenzene and 4-nitrotoluene were initially investigated as template reactions with selection of several terms such as different hydrogen source (H_2, HCOOH, etc.), different quantities of catalyst (from 2.5 to 12.5 wt.%) and different solvents (DMF, methanol, ethanol).

When using H_2 as a hydrogen source, the reaction system's pressure needs to be raised to several times of atmospheric pressure which would be quite dangerous. In comparison, HCOOH is good enough to use in the reaction as a hydrogen source while it only needs to be heated to 60°C which would not be a problem. The amount of the catalyst used is determined too. When using 3.64 wt.% (Pd-based) catalyst, the yield could reach the ideal level in a controllable time (generally 2 h). There was no significant rise in product's yield when adding more catalysts or using a product with more Pd loading to the system. As to the solvents, considering the temperature formic acid need and solubility, DMF was chosen to be used in the reaction.

Characterizations

Powder XRD patterns were recorded with $2\theta = 5–80°$ at a scan rate of 0.2°/s. Morphologic characterization was carried out by SEM (QUANTA FEG 250, FEI Company) and TEM (JEM-2100, JEOL Ltd., Japan). BET surface area, pore volume, and pore size were evaluated using nitrogen sorption experiments performed at 77 K on a Micromeritics ASAP 2020 adsorption apparatus, with the obtained isotherms analyzed using the built-in software. Elemental analysis was conducted using an Elementar Vario II analyzer (Elementar, German) in CHN mode, with combustion and reduction tube temperatures equaling 950°C and 500°C, respectively. HPLC was analyzed by ACQUITY UPLC H-Class.

Results and discussion

ZIF-67-US was fabricated (Scheme S1) with different stirring times and exposed to ultrasonic irradiation under different ultrasonication powers. With ultrasonic bath adding to the synthesizing system, yields of products were significantly improved.

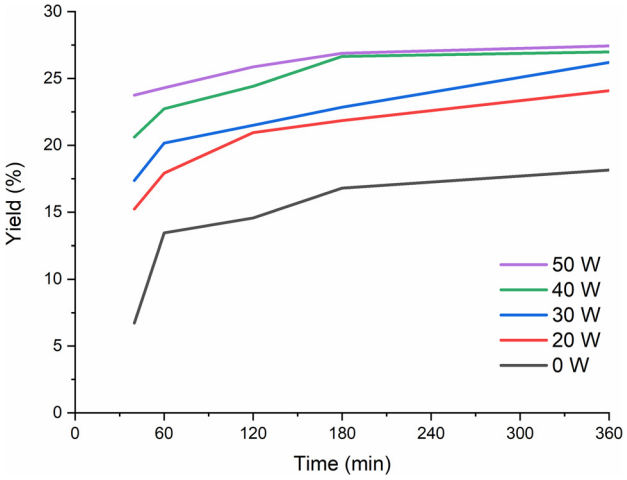


Figure 1. Yield of ultrasonic power result of synthesized ZIF-67-US (full power = 50 W, frequency = 40 kHz).

The formation and growth of ZIF frameworks were strongly influenced by ultrasonic irradiation. The assembling process of ZIF-67 was controlled by kinetic factors as ultrasonication accelerates mass transfer, resulting in a significant rise in the yield of ultrasonication-supported product in the first 30 min, with a negligible rise in temperature. As the power of ultrasonic irradiation increased, the overall yield of ZIF-67 was greatly improved, reaching the raise values of up to 150% (Fig. 1). Elementary analysis confirmed that ultrasonicated ZIF-67 contained 25.23 wt.% N, 42.17 wt.% C, and 4.53 wt.% H, in agreement with theoretical values of 25.11 wt.% N, 43.05 wt.% C, and 4.48 wt.% H. Detailed characterizations of the

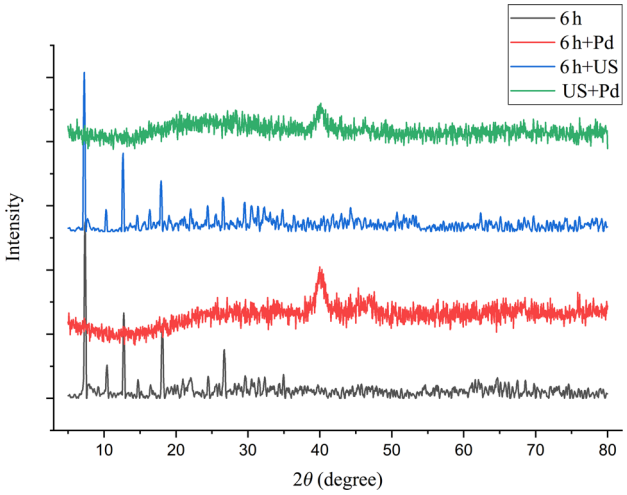


Figure 2. XRD diffraction patterns of Pd-loaded ZIF-67 and ZIF-67.

https://doi.org/10.1557/mrc.2018.183 Published online by Cambridge University Press

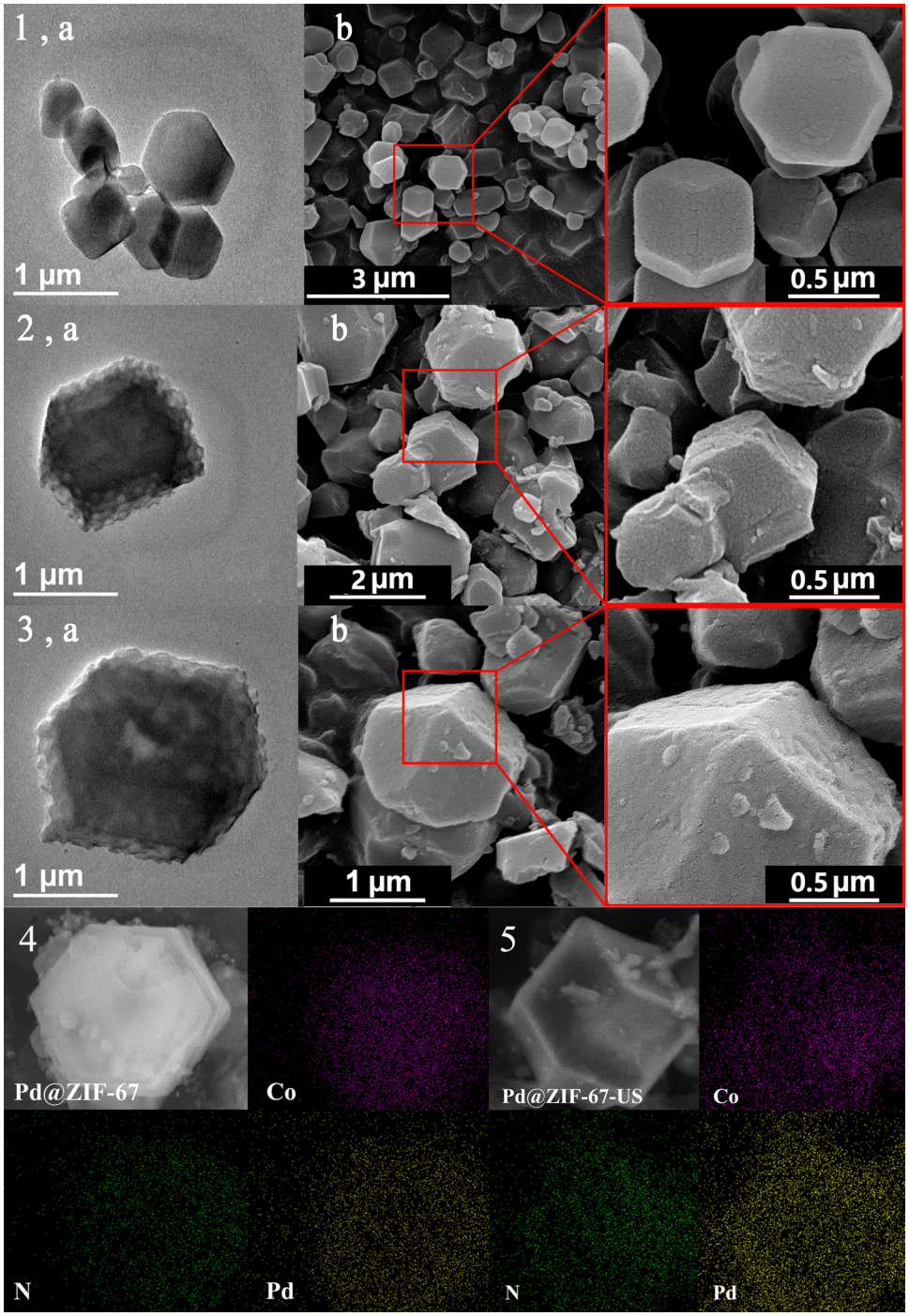


Figure 3. SEM, TEM images, and elemental mapping: (1–3) (a) TEM and (b) SEM images of ZIF-67 (6 h), ZIF-67-US (3 h), ZIF-67-US (6 h). (4–5) Elemental mapping of Pd–ZIF-67 and Pd–ZIF-67-US (40% of ultrasonication power, 6 h reaction time).

above compounds were performed by XRD, SEM, TEM, and N_2 sorption.

ZIF-67 and Pd-loaded ZIF-67 were synthesized under different conditions to determine the structural influence. The reaction time of ZIF-67 frameworks was varied from 10 min to 7 days. As shown in Figure S1, ZIF-67 frameworks started forming shortly after the injection of Co^{2+} into the 2-MeIm solution (peaks were already formed in 10 min), with the diffraction peaks of XRD pattern agree well with the standard pattern of ZIF-67. The crystal morphology remaining unchanged during the synthesizing process with ultrasonication as the diffraction peaks of the products remained the same from 10 min to

https://doi.org/10.1557/mrc.2018.183 Published online by Cambridge University Press

6 h and with ultrasonic irradiation. XDR pattern of ZIF-67-US showed a slightly weaker signal than ZIF-67 with the same reaction time of 6 h. As stated by Noori et al.,[33] ultrasonic irradiation is expected to afford products with increased mono-dispersity but decreased crystallinity, since the corresponding energy input causes structural collapse. In our work, both TG and SEM analyses showed no significant collapse in structure with ultrasonication. TG curve of ZIF-67-US confirmed the thermal stability is still good for over 300°C of decomposing temperature (Fig. S2).

After Pd NPs loaded onto ZIF-67, its original diffraction peaks disappeared, being replaced by strong characteristic peaks of Pd, which could be attributed to the diffraction peaks of Pd (JCPDS card No. 46-1043), suggesting the Pd NPs were grown along the direction[1] on the surface (Fig. 2). The gentle peaks suggest the defect inflicted to the crystal structure during Pd reduction and embedded processes which can be observed in SEM and TEM images.

SEM and TEM images clearly revealed the differences between conventional ZIF-67 and ultrasonication-treated ZIF-67-US. The smooth surface and perfect crystal structure of conventional ZIF-67 lead to strong XRD peaks but less Pd loading. Conversely, ultrasonication-treated Pd-ZIF-67-US showed a rougher and slightly collapsed surface suggesting the minor defects on the crystal structure surface but better Pd loading. Therefore, the SEM and TEM images not only explained the corresponding XRD patterns that showed no obvious crystal structure for both Pd-ZIF-67 and Pd-ZIF-67-US but also suggested the better Pd loading and catalytic performance in the reduction of organic pollutants that discussed later.

The images shown in Fig. 3 provided vital proof for explaining the advantage of ultrasonic treatment. As shown in Fig. 3 (1–3), ZIF-67 (6 h) comprised particles of approximately 0.78 μm in diameter with smooth surface and uniform size distribution. The pore size was found to be 2.12 nm and the pore volume was 0.56 cm^3/g. Ultrasonic irradiation-accelerated mass transfer leads to a much faster self-assembly and growth of the ZIF-67-US crystal. With ultrasonic irradiation for 3 h, the crystal has grown to the same level as the conventional method for 6 h. After 6 h ultrasonic irradiation, the framework has grown to approximately two times larger than conventional ones with the diameter approaching 1.65 μm, whereas the pore size and volume remain at the same level (2.11 nm and 0.59 cm^3/g).

Simultaneously, the outer surface of the ZIF-67 particles has become much rougher as the ultrasonic irradiation time and power increases, which leads to the differences in BET surface areas and Pd NPs distribution. Elemental mapping in Fig. 3 (4–5) reveals a better loading quality of ultrasonication-treated Pd-ZIF-67-US compared with the conventional Pd-ZIF-67 particles. The ultra-smooth outer surface of conventional ZIF-67 induces uneven Pd NPs distribution, featuring large empty areas and corner deposits which result in the low external surface area and poor catalytic activity. Conversely, Pd-ZIF-67-US showed a more even distribution of Pd NPs, results in the much higher external surface area and higher catalytic activity. The loading quantity of Pd is 2.44 wt.% (conventional Pd-ZIF-67) and 3.64 wt.% (Pd-ZIF-67-US), respectively (Fig. S3).

The textural features of ZIF-67 such as specific surface area and pore size were determined by N_2 adsorption–desorption isotherms (Fig. S4), revealing that BET surface areas of ultrasonicated products were higher than conventional ones, with being higher by 6.60% (non-loaded ZIF-67s) and 15.33% (Pd-loaded catalyst) separately. Ultrasonicated products exhibit more pores with diameters around 2 nm than the conventional ones which have more pores with larger sizes (Fig. S5).

Interestingly, the corresponding *t*-plot external surface areas, commonly used as a measurement of the external (large pore) surface area of microporous materials, showed pronounced differences, being 263.41% higher for ZIF-67-US and 63.37% higher for Pd-ZIF-67-US in comparison to the corresponding values of conventional ZIFs (Fig. 4). This increase was caused by higher surface roughness and larger volume of micropores, as shown in SEM images, favoring Pd NP attachment and thus benefitting the performance in catalytic reactions.

Incorporation of Pd on/in MOFs or ZIFs is widely studied in recent years. Lin et al. created a new core–shell structure of Pd/SiO_2–ZIF-8 composite which provides excellent product selectivity for the hydrogenations of alkenes.[34] Using a facile impregnation method, Pd NPs were supported onto ZIF-8 by Zhao et al. and the supported catalyst exhibits much higher activity than other supported MOFs.[35] Li et al. demonstrated the preparation of nano-sized yolk–shell Pd–ZIF-8 with excellent size selectivity in catalytic reactions.[36] Zhou and co-workers successfully fabricated Pd–ZIF-67 derivatives and compared their catalytic properties in Heck reaction.[37]

In order to meet the green chemistry concept, degradation of organic pollutants (e.g., nitrobenzene derivatives) was

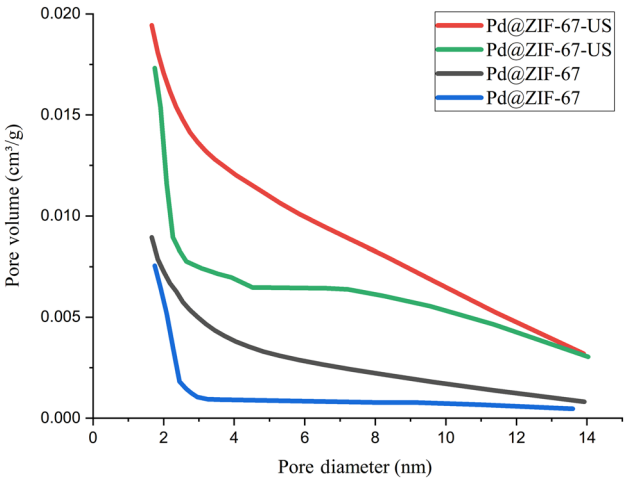
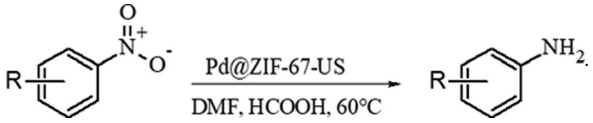
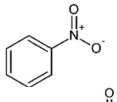
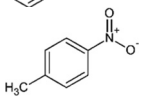
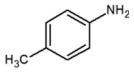
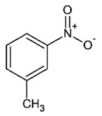
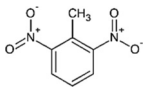
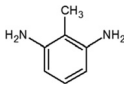
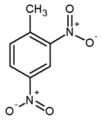
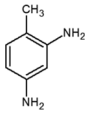
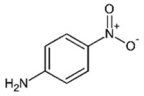
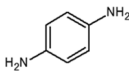
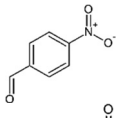
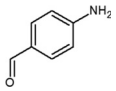
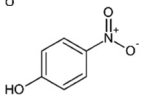
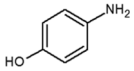
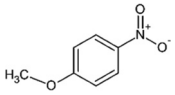
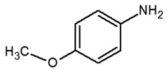
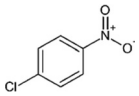
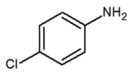
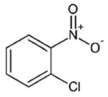
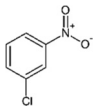
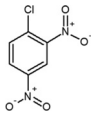
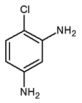


Figure 4. Pore volume distribution (adsorption and desorption) of conventional and ultrasonicated products.

https://doi.org/10.1557/mrc.2018.183 Published online by Cambridge University Press

Table 1. Hydrogenation of substituted aromatic nitro pollutants[a]



Entry	Substrate	Product	Time (h)	Yield (%)[b]	Yield (%)[c]
1			2	88	92
2			2	96	100
3			2	78	96
4			2	88	97
5			2	86	98
6			5	90	98
7			4	91	96
8			2	65	72
9			4	78	82
10			3	52	58
11			3	89	97
12			3	7	8
13			2	7	9

[a]Reaction conditions: reactant (2 mmol), DMF (20 mL), catalyst (20 mg), HCOOH (500 µL), 60°C.
[b]Using Pd–ZIF-67 as the catalyst.
[c]Using modified Pd–ZIF-67-US as the catalyst.

https://doi.org/10.1557/mrc.2018.183 Published online by Cambridge University Press

investigated in our study. Reaction conditions were optimized where the reduction of nitrobenzene and 4-nitrotoluene were initially investigated with different terms such as H_2 and HCOOH as a hydrogen source, DMF, and methanol as solvents. Finally, the reaction process was determined using HCOOH as the hydrogen source, 3.64 wt.% (based on Pd) of Pd–ZIF-67-US (40% of ultrasonication power, 6 h reaction time) as catalyst and DMF as the solvent. Under the optimized condition, we evaluated the performance of modified Pd–ZIF-67-US in catalytic reactions. The blank reaction was performed using nitrobenzene as a reactant with ZIF-67 and ZIF-67-US as catalysts where the other conditions remain the same as optimized. Both frameworks with no Pd loading exhibit the yield of 2%. With rougher surface and enhanced Pd NPs loading and larger external surface area, ultrasonicated catalyst exhibited an average of 9.7% performance improvement in reduction reaction to that of its conventional counterparts (Table I). The production selectivity of all the products with ultrasonicated catalysts are over 98% except 4-nitroanisole which was only 78%.

The heterogeneous reductions of nitrobenzene derivatives were affected by the chemical kinetics. Apart from concentration, temperature, pressure, and physical states of reactants, which were determined as the optimized conditions, the specific surface area of modified Pd–ZIF-67-US was the key to all the results. Smaller the particles and rougher the surfaces were, the larger surface can be involved in a reaction. Especially in the reactions of 2,4- and 2,6-dinitrotoluenes where the contact area of catalyst and reactant was larger for modified Pd–ZIF-67-US than conventional Pd–ZIF-67, resulting in the differences in initial reaction rate. Conversely, reactions of *m*/*p*-nitrotoluene were not affected by this factor, resulting in no obvious initial differences (Fig. S6).

In general, the reactions were hard to process when electron donor groups were in para-position (Table I, entries 6, 8, and 9) of the existing nitro group, or when electron-absorbent groups were in meta-position (Table I, entries 12 and 13) of the existing nitro group. It took more than double of the time for 4-nitroaniline and 4-nitrobenzaldehyde to be hydrogenated to a high yield. Meanwhile, 3-nitrochlorobenzene and 2,4-dinitrochlorobenzene can barely be reduced even when the reaction took more time (Table I, entries 12, 13; Fig. S5). All the reactions suggest a better catalytic performance of ultrasonication-modified catalyst.

To investigate the reusability, the ultrasonication-modified Pd–ZIF-67-US were recovered by centrifuging after each run, washed with methanol and acetone several times, and dried at 70°C overnight. The modified catalysts were used for at least five recycles to examine the catalytic activity. Due to the slight weight loss in the recovery process, we did several parallel experiments to make sure the recovered catalysts are enough (20 mg per experiment) until the fifth run. The modified catalyst retaining a high catalytic performance level of over 93% without a significant loss in the conversion of the optimized reaction condition (Fig. S7), revealing the excellent reusability of the catalysts.

Conclusions

In summary, new ultrasonication-supported synthesizing processes of Pd-free and Pd-loaded Co-based ZIFs (ZIF-67) have been developed. This work demonstrated a simple approach to the modification of existing supported catalyst. By introducing ultrasonic irradiation to the synthesizing process of the supported frameworks, the modified products exhibiting much better yields, larger BET-specific surface areas, and *t*-plot external surface areas. Moreover, the modified rougher surfaces caused by ultrasonication enhanced the loading of Pd NPs and increased the catalytic efficiency of the corresponding species in the reduction of aromatic nitro pollutants and the synthesized catalyst could be recycled and used for at least five times without significant loss in catalytic activity.

Supplementary material

The supplementary material for this article can be found at https://doi.org/10.1557/mrc.2018.183

Acknowledgment

The authors gratefully acknowledge the support by NSAF No. U1530101, NSFC No. 21771108, and No. 11702141.

References

1. H.-C. Li, W.-J. Liu, H.-X. Han, and H.-Q. Yu: Hydrophilic swellable metal–organic framework encapsulated Pd nanoparticles as an efficient catalyst for Cr(VI) reduction. *J. Mater. Chem. A* **4**, 11680 (2016).
2. X. Gu, Z.-H. Lu, H.-L. Jiang, T. Akita, and Q. Xu: Synergistic catalysis of metal–organic framework-immobilized Au–Pd nanoparticles in dehydrogenation of formic acid for chemical hydrogen storage. *J. Am. Chem. Soc.* **133**, 11822 (2011).
3. E.M. Banach, H.A. Stil, and H. Geerlings: Aluminium hydride nanoparticles nested in the porous zeolitic imidazolate framework-8. *J. Mater. Chem.* **22**, 324 (2012).
4. M. Mukoyoshi, H. Kobayashi, K. Kusada, M. Hayashi, T. Yamada, M. Maesato, J.M. Taylor, Y. Kubota, K. Kato, and M. Takata: Hybrid materials of Ni NP@ MOF prepared by a simple synthetic method. *Chem. Commun.* **51**, 12463 (2015).
5. B. Seoane, J.M. Zamaro, C. Tellez, and J. Coronas: Sonocrystallization of zeolitic imidazolate frameworks (ZIF-7, ZIF-8, ZIF-11 and ZIF-20). *CrystEngComm* **14**, 3103 (2012).
6. H.-Y. Cho, J. Kim, S.-N. Kim, and W.-S. Ahn: High yield 1-L scale synthesis of ZIF-8 via a sonochemical route. *Microporous Mesoporous Mater.* **169**, 180 (2013).
7. N. Jusoh, Y.F. Yeong, M. Mohamad, K.K. Lau, and A.M. Shariff: Rapid-synthesis of zeolite T via sonochemical-assisted hydrothermal growth method. *Ultrason. Sonochem.* **34**, 273 (2017).
8. S.A. Basnayake, J. Su, X. Zou, and K.J. Balkus Jr.: Carbonate-based zeolitic imidazolate framework for highly selective CO_2 capture. *Inorg. Chem.* **54**, 1816 (2015).
9. Q.-L. Zhu and Q. Xu: Metal–organic framework composites. *Chem. Soc. Rev.* **43**, 5468 (2014).
10. Y. Zare: Study of nanoparticles aggregation/agglomeration in polymer particulate nanocomposites by mechanical properties. *Compos. Part A Appl. Sci. Manuf.* **84**, 158 (2016).
11. S.A. Dergunov, M.D. Kim, S.N. Shmakov, A.G. Richter, S. Weigand, and E. Pinkhassik: Inside back cover: tuning optical properties of encapsulated clusters of gold nanoparticles through stimuli-triggered controlled aggregation (Chem. Eur. J. 23/2016). *Chem. Eur. J.* **22**, 7987 (2016).
12. P. Hervés, M. Pérez-Lorenzo, L.M. Liz-Marzán, J. Dzubiella, Y. Lu, and M. Ballauff: Catalysis by metallic nanoparticles in aqueous solution: model reactions. *Chem. Soc. Rev.* **41**, 5577 (2012).

https://doi.org/10.1557/mrc.2018.183 Published online by Cambridge University Press

13. E.T. Saka and Y. Çağlar: New Co(II) and Cu(II) phthalocyanine catalysts reinforced by long alkyl chains for the degradation of organic pollutants. *Catal. Letters* **147**, 1471 (2017).
14. W. Wu, M. Lei, S. Yang, L. Zhou, L. Liu, X. Xiao, C. Jiang, and V.A.L. Roy: A one-pot route to the synthesis of alloyed Cu/Ag bimetallic nanoparticles with different mass ratios for catalytic reduction of 4-nitrophenol. *J. Mater. Chem. A* **3**, 3450 (2015).
15. H. Fang, M. Wen, H. Chen, Q. Wu, and W. Li: Graphene stabilized ultrasmall CuNi nanocomposite with high activity and recyclability toward catalysing the reduction of aromatic nitro-compounds. *Nanoscale* **8**, 536 (2016).
16. F. Mojtabazade, B. Mirtamizdoust, A. Morsali, and P. Talemi: Sonochemical synthesis and structural determination of novel the nanocard house Cu(II) metal-organic coordination system. *Ultrason. Sonochem.* **35**, 226 (2017).
17. V. Belova, D.A. Gorin, D.G. Shchukin, and H. Möhwald: Selective ultrasonic cavitation on patterned hydrophobic surfaces. *Angew. Chem. Int. Ed.* **49**, 7129 (2010).
18. F. Israr, D. Chun, Y. Kim, and D.K. Kim: High yield synthesis of Ni-BTC metal-organic framework with ultrasonic irradiation: role of polar aprotic DMF solvent. *Ultrason. Sonochem.* **31**, 93 (2016).
19. F. Israr, D.K. Kim, Y. Kim, S.J. Oh, K.C. Ng, and W. Chun: Synthesis of porous Cu-BTC with ultrasonic treatment: effects of ultrasonic power and solvent condition. *Ultrason. Sonochem.* **29**, 186 (2016).
20. A. Nikseresht, A. Daniyali, M. Ali-Mohammadi, A. Afzalinia, and A. Mirzaie: Ultrasound-assisted biodiesel production by a novel composite of Fe (III)-based MOF and phosphotangestic acid as efficient and reusable catalyst. *Ultrason. Sonochem.* **37**, 203 (2017).
21. S.A.A. Razavi, M.Y. Masoomi, and A. Morsali: Ultrasonic assisted synthesis of a tetrazine functionalized MOF and its application in colorimetric detection of phenylhydrazine. *Ultrason. Sonochem.* **37**, 502 (2017).
22. S.S. Nadar and V.K. Rathod: Encapsulation of lipase within metal-organic framework (MOF) with enhanced activity intensified under ultrasound. *Enzyme Microb. Technol.* **108**, 11 (2018).
23. O. Abuzalat, D. Wong, M. Elsayed, S. Park, and S. Kim: Sonochemical fabrication of Cu(II) and Zn(II) metal-organic framework films on metal substrates. *Ultrason. Sonochem.* **45**, 180 (2018).
24. A.R. Abbasi, M. Karimi, and K. Daasbjerg: Efficient removal of crystal violet and methylene blue from wastewater by ultrasound nanoparticles Cu-MOF in comparison with mechanosynthesis method. *Ultrason. Sonochem.* **37**, 182 (2017).
25. L. Liang, Y. Tursun, A. Nulahong, T. Dilinuer, A. Tunishaguli, G. Gao, A. Abulikemu, and K. Okitsu: Preparation and sonophotocatalytic performance of hierarchical Bi 2 WO 6 structures and effects of various factors on the rate of Rhodamine B degradation. *Ultrason. Sonochem.* **39**, 93 (2017).
26. R.S. Vishwakarma and P.R. Gogate: Intensified oxalic acid crystallization using ultrasonic reactors: understanding effect of operating parameters and type of ultrasonic reactor. *Ultrason. Sonochem.* **39**, 111 (2017).
27. J. González-García, V. Sáez, I. Tudela, M.I. Díez-Garcia, M. Deseada Esclapez, and O. Louisnard: Sonochemical treatment of water polluted by chlorinated organocompounds. A review. *Water (Basel)* **2**, 28 (2010).
28. Y. Mu, Y. Zhang, J. Fan, and C. Guo: Effect of ultrasound pretreatment on the hydrothermal synthesis of SSZ-13 zeolite. *Ultrason. Sonochem.* **38**, 430 (2017).
29. F. Zhao and D. Cheng: Changes in pore size distribution inside sludge under various ultrasonic conditions. *Ultrason. Sonochem.* **38**, 390 (2017).
30. R.H. Jawale, A. Tandale, and P.R. Gogate: Novel approaches based on ultrasound for treatment of wastewater containing potassium ferrocyanide. *Ultrason. Sonochem.* **38**, 402 (2017).
31. J. Abdi, M. Vossoughi, N.M. Mahmoodi, and I. Alemzadeh: Synthesis of amine-modified zeolitic imidazolate framework-8, ultrasound-assisted dye removal and modeling. *Ultrason. Sonochem.* **39**, 550 (2017).
32. J. Qian, F. Sun, and L. Qin: Hydrothermal synthesis of zeolitic imidazolate framework-67 (ZIF-67) nanocrystals. *Mater. Lett.* **82**, 220 (2012).
33. Y. Noori, K. Akhbari, A. Phuruangrat, and F. Costantino: Studies the effects of ultrasonic irradiation and dielectric constants of solvents on formation of lead (II) supramolecular polymer; new precursors for synthesis of lead (II) oxide nanoparticles. *Ultrason. Sonochem.* **35**, 36 (2017).
34. L. Lin, T. Zhang, X. Zhang, H. Liu, K.L. Yeung, and J. Qiu: New Pd/SiO2@ZIF-8 core–shell catalyst with selective, antipoisoning, and anti-leaching properties for the hydrogenation of alkenes. *Ind. Eng. Chem. Res.* **53**, 10906 (2014).
35. Y. Zhao, M. Liu, B. Fan, Y. Chen, W. Lv, N. Lu, and R. Li: Pd nanoparticles supported on ZIF-8 as an efficient heterogeneous catalyst for the selective hydrogenation of cinnamaldehyde. *Catal. Commun.* **57**, 119 (2014).
36. F.L. Li, H.X. Li, and J.P. Lang: Fabrication of yolk–shell Pd@ZIF-8 nanoparticles with excellent catalytic size-selectivity for the hydrogenation of olefins. *Crystengcomm* **18**, 1760 (2016).
37. A. Zhou, R.M. Guo, J. Zhou, Y. Dou, Y. Chen, and J.R. Li: Pd@ZIF-67 derived recyclable Pd-based catalysts with hierarchical pores for high-performance heck reaction. *ACS Sustain. Chem. Eng.* **6**, 2103 (2018).

https://doi.org/10.1557/mrc.2018.183 Published online by Cambridge University Press